

DESY 96-147
 RAL-96-094
 November 1996

Associated $J/\psi + \gamma$ Photoproduction as a Probe of the Colour-Octet Mechanism

MATTEO CACCIARI^a, MARIO GRECO^b AND
 MICHAEL KRÄMER^c

^a*Deutsches Elektronen-Synchrotron DESY
 D-22603 Hamburg, Germany*

^b*INFN, Laboratori Nazionali di Frascati and
 Dipartimento di Fisica, Università di Roma III, Italy*

^c*Rutherford Appleton Laboratory
 Chilton, Didcot, OX11 0QX, England*

Abstract

The associated production of a J/ψ and a photon in photon-hadron collisions is considered, and shown to be a good probe of the presence of colour-octet mediated channels in quarkonia production, as predicted by the factorization approach within NRQCD. Total and differential cross sections for photoproduction at fixed target experiments and at HERA are presented. Associated $J/\psi + \gamma$ production at hadron colliders is briefly discussed.

PACS numbers: 13.60.-r, 13.60.Le, 13.85.Qk, 12.38.Bx

e-mail addresses: cacciari@desy.de
 greco@lnf.infn.it
 Michael.Kraemer@rl.ac.uk

1 Introduction

The study of heavy quarkonia production is a good testing ground for our understanding of the transition region between the realms of perturbative and non-perturbative Quantum Chromodynamics (QCD). Different production models have been devised, and all of them have to deal with the problem of properly describing and matching these two phases of QCD. Most recently the so-called Non Relativistic QCD (NRQCD) factorization approach (FA) has been proposed by Bodwin, Braaten and Lepage (BBL) [1]: an effective-field-theory framework in NRQCD is used to separate the short-distance scale of annihilation and production of heavy quarkonium from the long-distance scales associated to the quarkonium structure. A brief review of the various models is presented in section 2.

In particular the BBL approach (also referred to as FA) has been applied to describe quarkonia production at the Tevatron [2] providing a successful picture [3] of the production rates of J/ψ and ψ' - much larger than earlier predictions - which is related to the relevance of colour-octet contributions in the production mechanism. It is to be noted that this successful description relies on a certain number of non-perturbative parameters having to be fitted to the data. Therefore additional and more extensive comparisons with experimental data coming also from other kind of reactions are necessary to finally assess the validity of this approach. To this aim, calculations of inclusive quarkonia production in e^+e^- annihilation [4], Z decays [5], hadronic collisions at fixed-target experiments [6], B decays [7] and γp collisions (both for S -wave [8–11] and P -wave [12,13] states) have recently been performed within its frame. From refs. [8,10], in particular, the predictions based on the leading colour-octet contribution appear not to agree with recent experimental data obtained at HERA by the H1 Collaboration [14], indicating either a reduced phenomenological importance of the colour-octet terms than suggested by the Tevatron data analysis [3] or the possible relevance of higher order corrections.

In this paper we will consider the associated production of a J/ψ and a photon, where the photon has to be directly produced in the short-distance interaction, i.e. it should not come, for instance, from the radiative decay of a P -wave quarkonium into a J/ψ . This process therefore must have a very distinctive experimental signature, namely a J/ψ balanced in p_T by the hard photon. We will argue that the study of this reaction in γp collisions provides a powerful tool for assessing the importance of colour-octet terms

in quarkonia production. First results of our analysis have already been presented in [13].

The paper is organized as follows: in section 2 we will briefly review various quarkonia production models and the BBL approach. Then in section 3 we will introduce the basic diagrams which contribute to $J/\psi + \gamma$ photoproduction and discuss why this process provides a clear signature of colour-octet terms. Numerical results and Conclusions will follow in sects. 4 and 5 respectively.

2 Production Mechanisms

Any approach attempting to describe the production (or decay) of a heavy quarkonium must deal with two issues which - for sufficiently large quark masses - can be kept distinct: the production (or the annihilation) of the heavy quark-antiquark pair ($Q\bar{Q}$) constituting the quarkonium and their binding into a single physical long-lived particle. The heavy quark mass, $m_Q \gg \Lambda_{\text{QCD}}$, sets the scale for the short-distance interaction of producing or annihilating a $Q\bar{Q}$ pair, which can therefore be studied within perturbative QCD (pQCD) [15]. The binding of the two quarks into a bound state is on the other hand a long-distance process, and non-perturbative effects have to be included at this point. These are usually parametrized via form factors describing the probability of the $Q\bar{Q}$ pair to form the bound state. The degree of rigour, completeness and complexity of this sector varies greatly from approach to approach:

The Colour Evaporation Model (CEM) [16] rests on duality arguments [17] in assuming that $c\bar{c}$ pairs produced with an invariant mass below that of a $D\bar{D}$ mesons threshold, (taking charm as an example of heavy quark) will eventually hadronize into a charmonium state. Being this assumption only qualitative this model of course is unable to predict the production rate of a particular quarkonium state. It is therefore not very suitable for the study of exclusive final states.

The Colour Singlet Model (CSM) [18] tries to overcome this difficulty of the CEM by making a very precise request: the $Q\bar{Q}$ pair must be produced in the short-distance interaction with the same spin, angular momentum and colour quantum numbers of the quarkonium state. A single parameter, provided by the bound state Bethe-Salpeter wave function or its derivative, then describes the hadronization into the observable particle.

This model is of course much more predictive: the production rate for a colour-singlet $Q\bar{Q}$ state with a given spin and angular momentum, usually referred to as $Q\bar{Q}[2S+1L_J, \underline{1}]$, can be calculated exactly in pQCD. Moreover, the phenomenological parameter can be measured, for instance, in electromagnetic decays and used to make absolute predictions for production rates. Despite its physical transparency and predictive power, the CSM is clearly not a complete theory: It ignores, at least in its original formulation, relativistic corrections which take into account the nonzero relative velocity of quark and antiquark in the bound state. Moreover, there are no theorems that guarantee that the simple factorization of the quarkonium production cross section into a short-distance part and a single non-perturbative parameter is valid in higher orders of perturbation theory. In fact, in the case of hadronic production or decay of P -wave quarkonia, the radiative corrections to the short-distance cross section contain infrared divergences that cannot be factored into a single non-perturbative quantity. This failure is to be attributed to an incomplete description of the quarkonium wave function, in that the Colour Singlet Model ignores the contributions from higher Fock-state components. As a result, CSM predictions for producing J/ψ and ψ' states at large p_T have been found to grossly underestimate, by more than an order of magnitude, the experimental cross sections obtained by the CDF collaboration[2] in $p\bar{p}$ collisions at the Tevatron (see also [19] and references therein).

The factorization approach by Bodwin, Braaten and Lepage [1] provides a rigorous framework for treating quarkonium production and decays which resolves these problems. It extends the CSM by allowing $Q\bar{Q}$ pairs with spin, angular momentum and colour quantum numbers different from those of the observed quarkonium to hadronize into the latter. In this respect, the factorization formalism recovers some of the qualitative features of the CEM. The general expression for the production cross section within the NRQCD factorization approach reads

$$d\sigma(H + X) = \sum_n d\hat{\sigma}(Q\bar{Q}[n] + X) \langle \mathcal{O}^H[n] \rangle \quad (1)$$

Here $d\hat{\sigma}(Q\bar{Q}[n] + X)$ describes the short-distance production of a $Q\bar{Q}$ pair in the colour/spin/angular momentum state n , and $\langle \mathcal{O}^H[n] \rangle$, formally a vacuum expectation value of a NRQCD matrix element (see [1] for details), describes the hadronization of the $Q\bar{Q}$ pair into the observable quarkonium state H . One must note that the cross section is no more given by a single product of a

short-distance and a long-distance term as in the CSM, but rather by a sum of such terms. Infrared singularities which eventually show up in some of the short-distance coefficients would be absorbed into the long-distance part of other terms, thereby ensuring a well defined overall result. The relative importance of the various contributions in (1) can be estimated by using NRQCD velocity scaling rules [20]. For $v \rightarrow 0$ (v being the average velocity of the heavy quark in the quarkonium rest frame) each of the NRQCD matrix elements scales with a definite power of v and the general expression (1) can be organized into an expansion in powers of v^2 . For the production of S -wave bound states, like J/ψ , the colour-octet matrix elements associated with higher Fock state components in the quarkonium wave function are suppressed by a factor of v^4 compared to the colour-singlet contribution. The NRQCD description of S -wave quarkonia production or annihilation thus reduces to the Colour Singlet Model in the static limit $v = 0$.¹

However, completely ignoring the octet $Q\bar{Q}$ states, as in the CSM, can lead to too small quarkonium production cross sections whenever these states can be copiously produced in the short-distance interaction in comparison with the colour-singlet ones. This is the case for large- p_T J/ψ and ψ' production at the Tevatron. Indeed it has been found [3] that gluon production with subsequent fragmentation into a colour-octet 3S_1 $c\bar{c}$ pair (which will eventually hadronize into a physical quarkonium) can successfully describe the experimental data, greatly underestimated by the CSM. As will be demonstrated below, associated $J/\psi + \gamma$ photoproduction is a particularly sensitive probe of the NRQCD matrix element $\langle \mathcal{O}^{J/\psi}[{}^3S_1, 8] \rangle$ and will therefore provide an important consistency check of the colour-octet explanation of the high- p_T data at the Tevatron.

A recent review of the factorization approach and its applications to quarkonia production at colliders can be also found in ref. [22].

3 $J/\psi + \gamma$ Production

Associated $J/\psi + \gamma$ production has been studied in hadronic collisions by various authors over the recent years [23]. Kim and Reya [24] pointed out that $J/\psi + \gamma$ photo- and electroproduction represents a powerful tool for dis-

¹In the case of P -wave quarkonia, colour-singlet and colour-octet mechanisms contribute at the same order in v to annihilation rates and production cross sections and must therefore both be included for a consistent calculation [21].

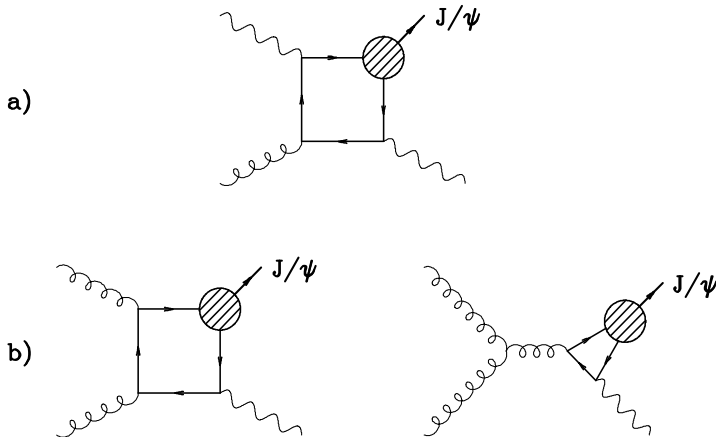


Figure 1: Diagrams contributing within the factorization approach to $J/\psi + \text{photon}$ associated production in direct (a) and resolved (b) photon collisions.

criminating between the Colour Evaporation Model and the Colour Singlet Model. The reason for this will be discussed below. Since all previous calculations were based on the Colour Singlet or Colour Evaporation Model it is worth to reconsider $J/\psi + \gamma$ production within the context of the new factorization approach. We will in fact demonstrate that this reaction is a particularly sensitive probe of the presence of colour-octet mediated channels in J/ψ production.

Before presenting our results within the BBL formalism, let us briefly review the reason why associated $J/\psi + \gamma$ production provides a good discrimination between the CEM and the CSM in photoproduction. Due to the colour constraint of the CSM, the leading order contribution, fig. 1a,

$$\gamma p \rightarrow \gamma + g_p \rightarrow c\bar{c}[{}^3S_1, \underline{1}] + \gamma \rightarrow J/\psi + \gamma \quad (2)$$

obviously vanishes in the Colour Singlet Model, since only one gluon is attached to the $c\bar{c}$ line. In order to allow for a second gluon one must either go to higher order in α_s for the direct photon process given above or consider a resolved photon process:

$$\gamma p \rightarrow g_\gamma + g_p \rightarrow c\bar{c}[{}^3S_1, \underline{1}] + \gamma \rightarrow J/\psi + \gamma \quad (3)$$

In both cases, we can expect a suppression of $J/\psi + \gamma$ photoproduction within the CSM. This is not the case in the CEM. Since the colour constraint is

absent, the process can proceed via the direct production channel giving a $c\bar{c}$ pair of invariant mass smaller than that of a $D\bar{D}$ pair threshold:

$$\gamma p \rightarrow \gamma + g_p \rightarrow c\bar{c}[M_{c\bar{c}} < M_{D\bar{D}}] + \gamma \rightarrow J/\psi + \gamma \quad (4)$$

Kim and Reya have indeed argued that at HERA within the CEM one should expect about a factor of five more $J/\psi + \gamma$ events than predicted by the CSM.

As stated before, the factorization approach shares some features of the CEM by allowing colour-octet intermediate states. For this case, in particular, it allows the $J/\psi + \gamma$ production to proceed also via direct photon interactions through a colour-octet $c\bar{c}$ pair. To be more specific, the following short-distance process can contribute:

Direct photon (fig. 1a):

$$\begin{aligned} \gamma + g_p &\rightarrow c\bar{c}[^1S_0, \underline{8}] + \gamma \\ \gamma + g_p &\rightarrow c\bar{c}[^3S_1, \underline{8}] + \gamma \\ \gamma + g_p &\rightarrow c\bar{c}[^3P_J, \underline{8}] + \gamma \end{aligned}$$

Resolved photon (fig. 1b):

$$\begin{aligned} g_\gamma + g_p &\rightarrow c\bar{c}[^1S_0, \underline{8}] + \gamma \\ g_\gamma + g_p &\rightarrow c\bar{c}[^3S_1, \underline{1}] + \gamma \quad (\text{Standard CSM process}) \\ g_\gamma + g_p &\rightarrow c\bar{c}[^3S_1, \underline{8}] + \gamma \\ g_\gamma + g_p &\rightarrow c\bar{c}[^3P_J, \underline{8}] + \gamma \end{aligned}$$

Light-quark initiated processes are strongly suppressed and can safely be neglected. Resolved production of a colour-singlet χ_J state and a hard photon, with the χ_J , radiatively decaying into J/ψ plus an unobserved soft photon, could constitute a background to our signal, but turns out to be zero.

According to the NRQCD velocity scaling rules [20] and fits to the Tevatron data [3] the colour-octet non-perturbative matrix elements that enter associated $J/\psi + \gamma$ production should be suppressed by about two orders of magnitude compared to the colour-singlet matrix element. Still, however, the two following features can be qualitatively expected:

- i) the production of colour-octet states via a direct process - rather than a resolved one - will at least partially compensate for the smaller matrix elements. We should therefore expect a sizable increase in the overall cross section due to colour-octet channels;

- ii) the distribution in the inelasticity of the J/ψ , namely the ratio of its energy over the initial photon energy in the proton rest frame, usually indicated with z (in a generic frame $z = p_{J/\psi} \cdot p_p / p_\gamma \cdot p_p$), will be more peaked towards one for the colour-octet induced processes. This is again due to the presence of a direct photon coupling as opposed to the resolved one, where the g_γ only carries part of the photon energy into the reaction.

These qualitative features are in fact born out by our numerical analysis to be presented and discussed in the next section. The parton cross sections (5) have been evaluated using the algebraic computer program FORM [25]. We note here that the direct photon diagram in fig. 1a happens to contribute to $[^3S_1, 8]$ production only. Moreover, due to the triple gluon vertex in the second diagram of fig. 1b, the cross sections for the resolved photon contribution to 1S_0 and $^3P_{0,2}$ octet states display a collinear and infrared singularity in the $p_T = 0$ and $z = 1$ endpoint. Rather than properly subtracting it we will avoid this phase space region by applying a minimum- p_T cut.

4 Numerical Results

The numerical results have been obtained by adopting the following set of parameters. As for the strong coupling, we employ the leading order formula

$$\alpha_s(\mu) = \frac{12\pi}{(33 - 2n_f) \ln(\mu^2/\Lambda^2)} \quad (5)$$

with $n_f = 4$ and $\Lambda_{LO}^{(4)} = 120$ MeV. The scale μ has been taken equal to the transverse J/ψ mass, namely $\mu = M_T = \sqrt{4m_c^2 + p_T^2}$, and the charm mass m_c has been taken equal to 1.5 GeV. For both the proton and the resolved photon structure functions the GRV92 leading order parton densities [26] have been employed, evaluated at the factorization scale $\mu_F = M_T$.

Finally, the non-perturbative matrix elements have been fixed to values compatible with both the NRQCD scaling rules and with the Tevatron fits, as in ref. [8]. Their values are summarized in Table 1.

We first compare the total cross sections given by the various production channels, with a fixed $p_T > 1$ GeV cut applied to avoid the infrared/collinear singularities in some of the cross sections. Table 2 shows the results for a) γp collisions in a fixed target set-up, with an incoming photon energy of 100

$\langle \mathcal{O}^{J/\psi} [{}^3S_1, \underline{1}] \rangle$	1.16 GeV ³	$m_c^3 v^3$
$\langle \mathcal{O}^{J/\psi} [{}^1S_0, \underline{8}] \rangle$	10^{-2} GeV ³	$m_c^3 v^7$
$\langle \mathcal{O}^{J/\psi} [{}^3S_1, \underline{8}] \rangle$	10^{-2} GeV ³	$m_c^3 v^7$
$\langle \mathcal{O}^{J/\psi} [{}^3P_0, \underline{8}] \rangle / m_c^2$	10^{-2} GeV ³	$m_c^3 v^7$

Table 1: Values of the NRQCD matrix elements used in the numerical analysis, with the velocity and mass scaling. v is the velocity of the heavy quark in the quarkonium rest frame. For charmonium it holds $v^2 \simeq 0.23$. It also holds $\langle \mathcal{O}^{J/\psi} [{}^3P_J, \underline{8}] \rangle \simeq (2J+1) \langle \mathcal{O}^{J/\psi} [{}^3P_0, \underline{8}] \rangle$.

GeV; b) γp collisions at a center of mass energy of 100 GeV and c) HERA kinematics, i.e. 27.5 GeV electron and 820 GeV proton collisions. For the case c) the electroproduction cross sections have been evaluated by averaging the photoproduction ones weighted by the usual Weizsäcker-Williams flux factor,

$$\sigma_{ep}(s) = \int_{y_{min}}^{y_{max}} dy f_{\gamma/e}(y) \sigma_{\gamma p}(ys) \quad (6)$$

with

$$f_{\gamma/e}(y) = \frac{\alpha}{2\pi} \left[\frac{1 + (1-y)^2}{y} \ln \frac{Q_{max}^2}{Q_{min}^2} + 2m_e^2 y \left(\frac{1}{Q_{max}^2} - \frac{1}{Q_{min}^2} \right) \right] \quad (7)$$

where $y = E_\gamma/E_e$, $Q_{min}^2 = m_e^2 y / (1-y)$ and m_e is the electron mass. We adopt $Q_{max}^2 = 4$ GeV² and $y_{min} = 0.15$, $y_{max} = 0.86$ according to [27].

The results presented in Table 2 clearly show that in a typical fixed target set-up, with a photon beam energy of 100 GeV, the cross section is dominated by the direct photon production of a colour-octet 3S_1 state. Although the cross section is small, the observation of this process at fixed-target experiments would therefore already provide good evidence for the importance of colour-octet contributions.

At a higher center of mass energy, on the other hand, the production of a J/ψ via a colour-singlet 3S_1 state in resolved photon collisions and via a colour-octet 3S_1 state in direct photon collisions represents the major part of the cross section. The numbers presented in Table 2 indicate that at HERA energies colour-octet channels could amount to about 40% of the overall production rate. The presence of colour-octet contributions can however not be assessed from total cross sections alone, given the large normalization uncertainties present in the calculation from higher order corrections, parton

Channel		γp $E_\gamma = 100 \text{ GeV}$ $p_T > 1 \text{ GeV}$	γp $\sqrt{s} = 100 \text{ GeV}$ $p_T > 1 \text{ GeV}$	ep $\sqrt{s} = 300 \text{ GeV}$ $p_T > 1 \text{ GeV}$	ep $\sqrt{s} = 300 \text{ GeV}$ $p_T > 1 \text{ GeV}$ $-3 < \eta < 3$ $E_\gamma > 2 \text{ GeV}$
Direct	$^1S_0, \underline{8}$	—	—	—	—
	$^3S_1, \underline{8}$.48	7.67	.63	.44
	$^3P_J, \underline{8}$	—	—	—	—
Resolved	$^1S_0, \underline{8}$.0013	.35	.044	.020
	$^3S_1, \underline{1}$.072	16.70	2.05	.75
	$^3S_1, \underline{8}$.0012	.27	.033	.012
	$^3P_0, \underline{8}$.0046	1.03	.13	.048
	$^3P_1, \underline{8}$.0005	.14	.018	.007
	$^3P_2, \underline{8}$.0045	.97	.12	.043

Table 2: Results for the total cross sections (in pb). Notice that while in the first data column E_γ refers to the incoming photon beam energy in the last one it refers instead to the produced outgoing photon.

distribution functions and charm quark mass values, as well as unknown higher-twist contributions.

Therefore, we propose to study differential distributions to disentangle the colour-octet contributions from the standard colour-singlet one.

In fig. 2 we show the differential distributions related to the total γp cross sections at $\sqrt{s} = 100 \text{ GeV}$ with a minimum- p_T cut of 1 GeV, presented in Table 2. The distributions due to colour-singlet $[^3S_1, \underline{1}]$ production in resolved photon collisions (continuous line) and to colour-octet $[^3S_1, \underline{8}]$ production in direct photon collisions (dashed line) only are shown. The distributions due to the other colour-octet processes do indeed present the same features as the ones of $[^3S_1, \underline{1}]$, being also produced in resolved photon interactions, but are suppressed in magnitude, as can be seen from Table 2. Their inclusion would therefore not change the picture we are going to discuss.

As expected, the effect of the colour-octet $[^3S_1, \underline{8}]$ contribution produced in direct photon processes can easily be seen in at least some of the plots. While the p_T of the J/ψ and the invariant mass distribution M of the J/ψ - γ pair are pretty similar for the colour-singlet and colour-octet induced channels, the z , rapidity and photon energy distributions do indeed show a strikingly different behaviour.

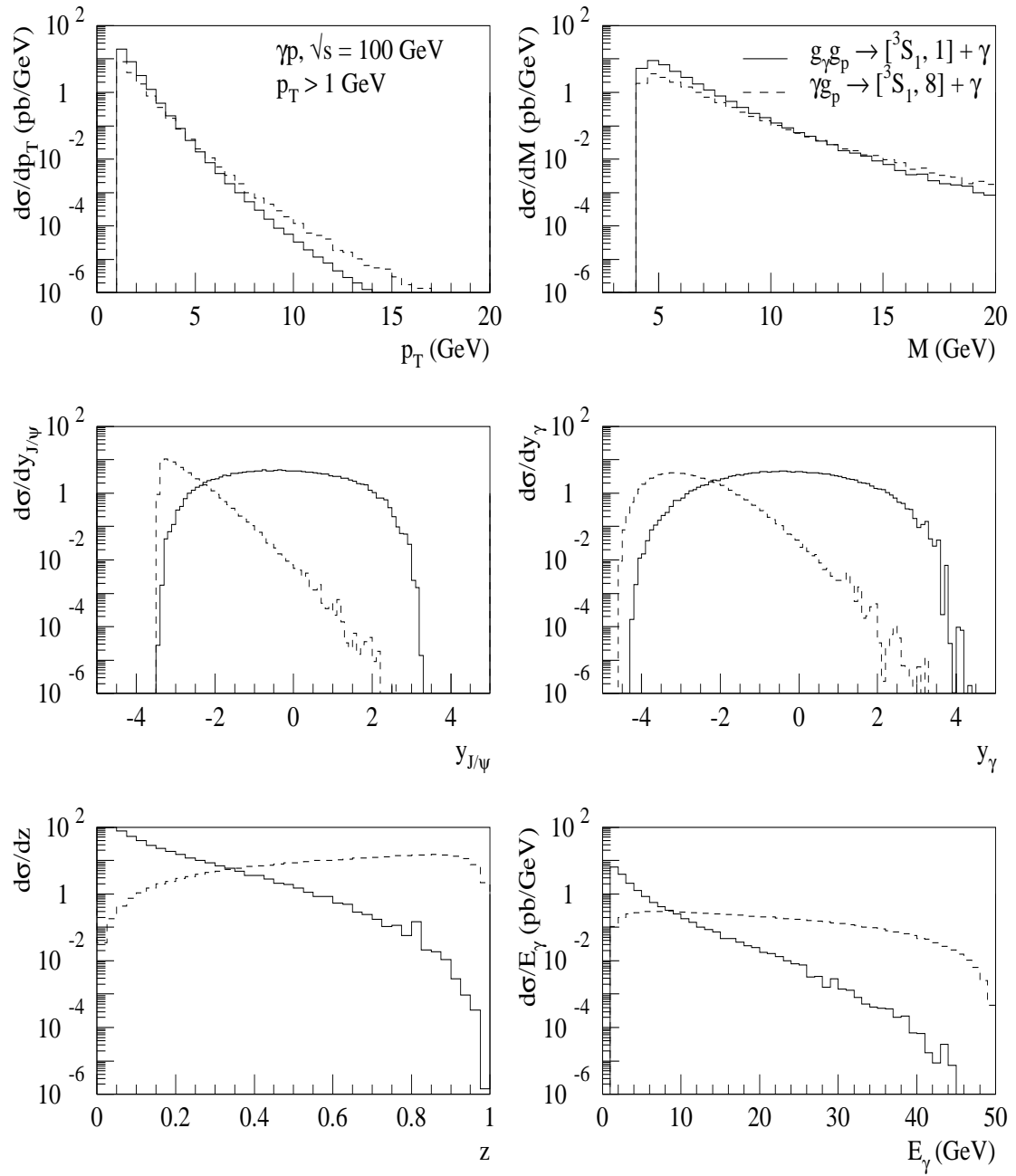


Figure 2: Differential distributions in γp collision at $\sqrt{s} = 100$ GeV. A minimum- p_T cut of 1 GeV is applied.

Recalling that we put ourselves in the so-called “HERA-frame”, with the photon (or the electron) traveling in the direction of negative rapidities, we notice how the direct photon coupling favours the production of the quarkonium and of the photon in the negative rapidities region. This contrasts the case of resolved photon production of colour-singlet 3S_1 states, which are uniformly produced around the central rapidity region.

As for the z distribution, the resolved photon process predicts a decrease of the cross section going towards the high- z region.. The direct photon process does on the other hand predict the opposite behaviour: the cross section now increases going towards $z = 1$. The small dip in the last few bins is due to the minimum- p_T cut.

The photon energy distribution behaves similarly to the z distribution, and is predicted to be much harder in direct photon processes.

The above distributions (the shapes of which have been checked to be robust with respect to a higher p_T cut, to be sure of the absence of p_T^{min} effects) provide a clear experimental signature; in particular the observation of a substantial fraction of $J/\psi + \gamma$ events in the high- z region would already be good evidence for the presence of colour-octet contributions to the J/ψ production cross section.

However, since actually HERA provides electron-proton interactions, we are going to investigate how the distributions look like in this frame. For consistency, we will first consider, in fig. 3, the differential cross section corresponding to the total ep cross section shown in Table 2. Successively, the effect of some experimental-like cuts will be taken into account.

Comparing fig. 3 with fig. 2 we notice that, due to the system being now boosted in the proton direction (i.e. positive rapidities), the non Lorentz invariant observables are affected. More precisely, the rapidity distributions of both the J/ψ and of the photon are slightly smeared and shifted towards positive rapidities. The largest difference can however be observed in the photon energy distributions: the one due to the resolved photon process is hardened with respect to γp interactions, while the one due to direct photon interaction is greatly softened. This can be understood assuming that most of the very energetic photons in direct photon collisions are produced in the incoming photon direction (see the rapidity distribution). The effect of a boost of the event in the opposite direction will then soften this distribution. In resolved photon interactions, on the other hand, events of this kind are produced more uniformly around the central rapidity region, and the boost will then also harden at least part of them.

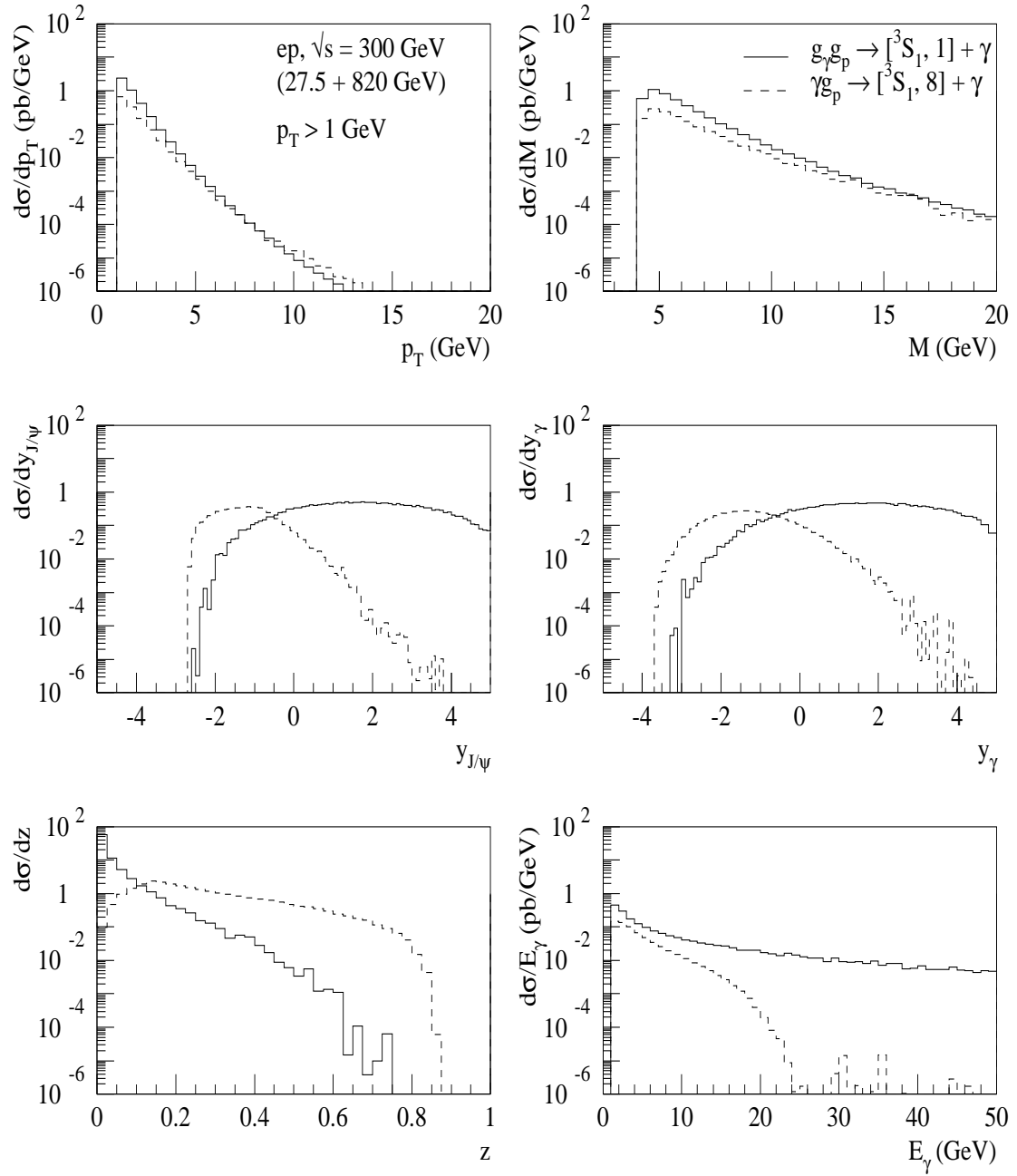


Figure 3: Differential distributions in ep collision at $\sqrt{s} = 300$ GeV. A minimum- p_T cut of 1 GeV is applied.

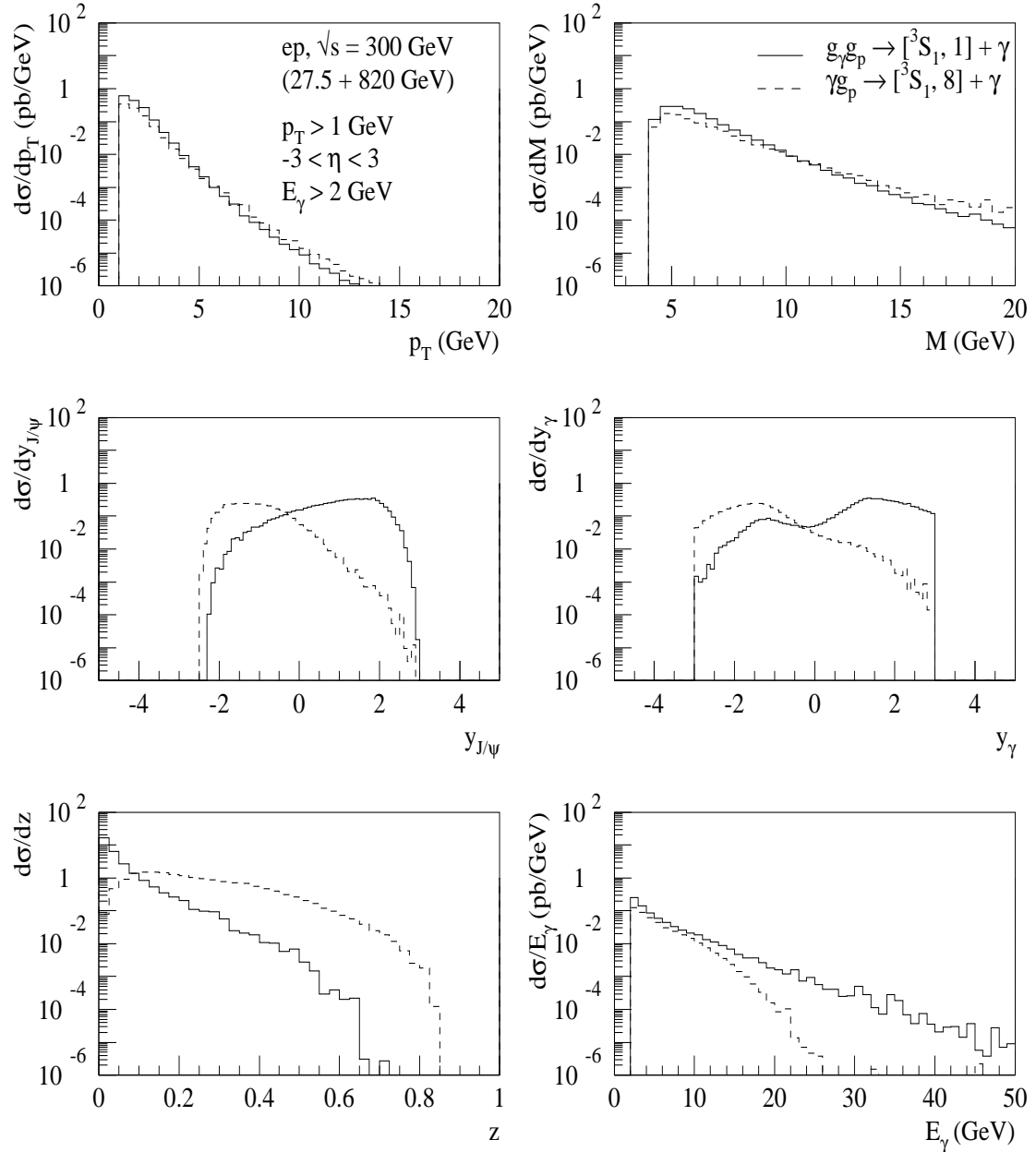


Figure 4: Differential distributions in ep collision at $\sqrt{s} = 300$ GeV. A minimum- p_T cut of 1 GeV, a minimum outgoing photon energy cut of 2 GeV and a pseudorapidity cut $|\eta_{J/\psi, \gamma}| < 3$ are applied.

The effect of applying some realistic experimental cuts can be appreciated in fig. 4. Since the produced photon must be clearly visible in the event, it is now required to lie (together with the J/ψ) within the pseudorapidity region $|\eta| < 3$ and to have an energy, in the lab frame, greater than 2 GeV. This last requirement also ensures that it will not be mistaken with a photon coming from the radiative decay of a P -wave state to a J/ψ , having energies of a few hundreds MeV. A further experimental selection criterion to exclude radiative decays photons consists in asking the photon p_T to be roughly opposite to that of the J/ψ . The distributions of fig. 4 are qualitatively similar to the ones - without cuts - of fig. 3, showing that colour-octet contributions in associated $J/\psi + \gamma$ electroproduction should be visible in the photon fragmentation region (negative rapidities in the HERA frame) or, more clearly, in the large- z region.

5 $J/\psi + \gamma$ in hadron collisions

Before closing, it is worth noticing that the resolved processes of fig. 1b also contribute to the associated $J/\psi + \gamma$ production in hadron collisions. To check whether a signature for colour-octet mediated processes can be seen at a hadron collider we have evaluated the total $J/\psi + \gamma$ cross section in $p\bar{p}$ collisions at $\sqrt{s} = 1800$ GeV. Light-quark initiated processes are suppressed and have been neglected. The following cuts have been imposed:

$$p_T > 4 \text{ GeV}, \quad |\eta_{J/\psi, \gamma}| < 0.6, \quad E_\gamma > 2 \text{ GeV} \quad (8)$$

The results are displayed in Table 3. The colour-octet terms can be seen to enhance the cross section by about 50%. However, given the large normalization uncertainties involved and the fact that the differential distributions in this case do not differ substantially from the colour-singlet process' ones, we conclude that there is little hope to shed light on the colour-octet mechanism via $J/\psi + \gamma$ production in hadron collisions.

6 Conclusions

The associated $J/\psi + \gamma$ production in ep and γp collisions has been proposed as a powerful tool for establishing the presence of quarkonia production processes mediated by colour-octet $Q\bar{Q}$ states, as suggested by the factorization approach of Bodwin, Braaten and Lepage.

Channel	$\sigma_{p\bar{p}}(J/\psi + \gamma)$ (pb) $\sqrt{s} = 1800$ GeV $p_T > 4$ GeV $ \eta_{J/\psi, \gamma} < 0.6$ $E_\gamma > 2$ GeV
$^3S_1, \underline{1}$	93.2
$^1S_0, \underline{8}$	12.3
$^3S_1, \underline{8}$	1.5
$^3P_0, \underline{8}$	10.0
$^3P_1, \underline{8}$	13.8
$^3P_2, \underline{8}$	7.7

Table 3: Results for the total cross sections in hadron collisions (in pb).

The very fact that colour-octet contributions to $J/\psi + \gamma$ photoproduction can proceed also via a direct photon coupling rather than via a resolved one only - as for the colour-singlet channel - leads to clean experimental signatures. We have shown that at HERA energies the colour-octet terms can increase the cross section by about 50% and, most importantly, produce a J/ψ energy distribution $d\sigma/dz$ strikingly different from the one predicted by the colour-singlet channel alone.

The hadroproduction case, taking the Tevatron as an example, has also been investigated. This cross section is also increased by about 50% by octet terms, but no significant signatures in differential distributions can be found.

Note added: After completion of our work an analysis of colour-octet contributions to associated $J/\psi + \gamma$ production in hadron-hadron collisions appeared [28]. After correcting what is probably a trivial misprint in the labelling of figs. 6-8 of [28] (they should have units nb rather than pb), their results are consistent with ours.

References

[1] G.T. Bodwin, E. Braaten and G.P. Lepage, Phys. Rev. **D51** (1995) 1125

- [2] F. Abe *et al.* (CDF Coll.), Phys. Rev. Lett. **69** (1992) 3704, Phys. Rev. Lett. **71** (1993) 2537, FERMILAB-CONF-96/156-E
- [3] E. Braaten and S. Fleming, Phys. Rev. Lett. **74** (1995) 3327
 M. Cacciari, M. Greco, M.L. Mangano and A. Petrelli, Phys. Lett. **B356** (1995) 560
 P. Cho and A.K. Leibovich, Phys. Rev. **D53** (1996) 150 and Phys. Rev. **D53** (1996) 6203
 M. Cacciari and M. Greco, Phys. Rev. Lett. **73** (1994) 1586
 E. Braaten, M.A. Doncheski, S. Fleming and M.L. Mangano, Phys. Lett. **B333** (1994) 548
 D.P. Roy and K. Sridhar, Phys. Lett. **B339** (1994) 141
- [4] E. Braaten and Y.-Q. Chen, Phys. Rev. Lett. **76** (1996) 730
- [5] K. Cheung, W.-Y. Keung and T.C. Yuan, Phys. Rev. Lett. **76** (1996) 877
 P. Cho, Phys. Lett. **B368** (1996) 171
- [6] W.-K. Tang and M. Vänttinen, Phys. Rev. **D53** (1996) 4851 and Phys. Rev. **D54** (1996) 4349
 S. Fleming and I. Maksymyk, Phys. Rev. **D54** (1996) 3608
 S. Gupta and K. Sridhar, Phys. Rev. **D54** (1996) 5545
 M. Beneke and I.Z. Rothstein, Phys. Rev. **D54** (1996) 2005
- [7] P. Ko, J. Lee, and H.S. Song, Phys. Rev. **D53** (1996) 1409
 S. Fleming, O.F. Hernández, I. Maksymyk and H. Nadeau, MADPH-96-953 (hep-ph/9608413)
- [8] M. Cacciari and M. Krämer, Phys. Rev. Lett. **76** (1996) 4128
- [9] J. Amundson, S. Fleming and I. Maksymyk, UTTG-10-95 (hep-ph/9601298)
- [10] P. Ko, J. Lee and H.S. Song, Phys. Rev. **D54** (1996) 4312
- [11] R. Godbole, D.P. Roy, and K. Sridhar, Phys. Lett. **B373** (1996) 328
- [12] J.P. Ma, Nucl. Phys. **B460** (1996) 109

- [13] M. Cacciari and M. Krämer, Proceedings of the workshop *Future Physics at HERA*, Vol 1, p. 416, eds. G. Ingelman, A. De Roeck and R. Klanner (hep-ph/9609500)
- [14] S. Aid *et al.* (H1 Coll.), Nucl. Phys. **B472** (1996) 3. See also M. Derrick *et al.* (ZEUS Coll.), presented by L. Stanco at the International Workshop on Deep Inelastic Scattering, Rome, April 1996
- [15] J.C. Collins, D.E. Soper and G. Sterman, Nucl. Phys. **B263** (1986) 37
- [16] H. Fritzsch, Phys. Lett. **67B** (1977) 217
 F. Halzen, Phys. Lett. **69B** (1977) 105
 F. Halzen and S. Matsuda, Phys. Rev. **D17** (1978) 1344
 M. Glück, J. Owens and E. Reya, Phys. Rev. **D17** (1978) 2324
- [17] A. Bramon, E. Etim and M. Greco, Phys. Lett. **41B** (1972) 609
- [18] E.L. Berger and D. Jones, Phys. Rev. **D23** (1981) 1521
 R. Baier and R. Rückl, Phys. Lett. **102B** (1981) 364
 for a recent review see also G.A. Schuler, CERN-TH.7170/94 (hep-ph/9403387)
- [19] M.L. Mangano, in *Tenth Topical Workshop on Proton-Antiproton Collider Physics*, eds. R. Raja and J. Yo (American Institute for Physics, 1995), CERN-TH-95-190 (hep-ph/9507353)
- [20] G.P. Lepage, L. Magnea, C. Nakhleh, U. Magnea and K. Hornbostel, Phys. Rev. **D46** (1992) 4052
- [21] G.T. Bodwin, E. Braaten and G.P. Lepage, Phys. Rev. **D46** (1992) R1914
- [22] E. Braaten, S. Fleming and T.C. Yuan, OHSTPY-HEP-T-96-001 (hep-ph/9602374)
- [23] M. Drees and C.S. Kim, Z. Phys. **C53** (1992) 673
 K. Sridhar, Phys. Lett. **B289** (1992) 435
 R.V. Gavai, R.M. Godbole and K. Sridhar, Phys. Lett. **B299** (1993) 157
 K. Sridhar, Phys. Rev. Lett. **70** (1993) 1747
 E.L. Berger and K. Sridhar, Phys. Lett. **B317** (1993) 443

M.A. Doncheski and C.S. Kim, Phys. Rev. **D49** (1994) 4463
C.S. Kim and E. Mirkes, Phys. Lett. **B346** (1994) 124 and Phys. Rev.
D51 (1995) 3340
D.P. Roy and K. Sridhar, Phys. Lett. **B341** (1995) 413
H.A. Peng, Z.M. He and C.S. Ju, Phys. Lett. **B351** (1995) 349

- [24] C.S. Kim and E. Reya, Phys. Lett. **B300** (1993) 298
- [25] FORM 2.0 by J.A.M. Vermaseren, CAN, Amsterdam, 1991
- [26] M. Glück, E. Reya, and A. Vogt, Phys. Rev. **D46** (1992) 1973, Z. Phys. **C53** (1992) 127 and Z. Phys. **C67** (1995) 433
- [27] M. Derrick *et al.* (ZEUS Coll.), Phys. Lett. **B349** (1995) 225
- [28] C.S. Kim, J. Lee, and H.S. Song, KEK-TH-474 (hep-ph/9610294)